Research Article

Ray Tracing RF Field Prediction: An Unforgiving Validation

**E. M. Vitucci,[1] V. Degli-Esposti,[2] F. Fuschini,[1] J. S. Lu,[2]
M. Barbiroli,[1] J. N. Wu,[2] M. Zoli,[1] J. J. Zhu,[2] and H. L. Bertoni[3]**

[1]*Dipartimento di Ingegneria dell'Energia Elettrica e dell'Informazione "Guglielmo Marconi", Alma Mater Studiorum,
Università di Bologna, 40136 Bologna, Italy*
[2]*Polaris Wireless Inc., 301 North Whisman Road, Mountain View, CA 94043, USA*
[3]*NYU Wireless Center of Polytechnic School of Engineering, New York University, Brooklyn, NY 11201, USA*

Correspondence should be addressed to E. M. Vitucci; enricomaria.vitucci@unibo.it

The prediction of RF coverage in urban environments is now commonly considered a solved problem with tens of models proposed in the literature showing good performance against measurements. Among these, ray tracing is regarded as one of the most accurate ones available. In the present work, however, we show that a great deal of work is still needed to make ray tracing really unleash its potential in practical use. A very extensive validation of a state-of-the-art 3D ray tracing model is carried out through comparison with measurements in one of the most challenging environments: the city of San Francisco. Although the comparison is based on RF cellular coverage at 850 and 1900 MHz, a widely studied territory, very relevant sources of error and inaccuracy are identified in several cases along with possible solutions.

1. Introduction

Deterministic prediction of radio frequency (RF) coverage, or received signal strength indicator (RSSI), in urban environment has been widely addressed during the last 20 years, in particular through ray-based propagation models. Making use of the ray-optical approximation originally developed for optical propagation problems [1] and of theories to describe diffraction problems [2], ray-based propagation models such as ray tracing describe the propagating field as a set of rays undergoing multiple reflections and diffractions over and around the obstacles (e.g., terrain and buildings) in the propagation environment.

Although ray tracing models have been shown to be the most accurate deterministic models available if properly fed a detailed description of the environment (e.g., building database), their widespread application has been hindered by the high complexity of operation and high computation time. For this reason, several methods to limit the number of propagating rays have been proposed over the years.

Multiple-diffraction models for over-roof-top propagation in the radial direction have been developed for macro cells [3] and two-dimensional (2D) models accounting for reflections and diffractions in the horizontal plane have been proposed for microcells [4]. Propagation in complex environments has been modelled with more sophisticated quasi-3D ray tracing (RT) approaches [5], or using fully 3D algorithms [6, 7]. More recently diffuse scattering phenomena due to irregularities of building walls have been embedded in ray tracing models to improve prediction accuracy [8, 9].

However, within most studies, validation was performed using a limited set of measurement data in a few reference environments. Typically, each set had less than a few hundred points. This is mainly due to the limited number of available measurements and to the high computation time involved in ray tracing operation. Furthermore, the measurement campaigns were often carried out at night to minimize the effect of traffic, and avoiding vegetated or hilly areas and very irregular urban layouts. To the authors' knowledge, only one study addressed large-scale RF coverage prediction under normal operating conditions [10].

In the present paper the approach has been reversed: starting from an extensive and complete set of measurements in a challenging environment related to a practical

application, the actual performance of ray tracing has been assessed in a fair and complete way. A state-of-the-art 3D RT model including diffuse scattering is validated for the first time against a large set of measurements recorded in one of the most challenging environments: the city of San Francisco, USA. This set considers 18 transmitting base station sites and thousands of receivers per site with link distances ranging from a few meters to some kilometres. The San Francisco environment is characterized by an extreme variety of buildings from small wooden houses to 250 m tall glass-and-steel skyscrapers, a very hilly terrain, and a widespread presence of vegetation traffic, bridge ramps, and freeway junctions within the urban layout.

In this investigation the measurement versus prediction comparison is based on narrowband RF coverage at 850 and 1900 MHz. Although it might appear old-fashioned, RF coverage is still the most important radio propagation parameter for the performance of present and future wireless communication systems, as well as for the implementation of RF-based services such as RSSI-based fingerprinting localization techniques for emergency and surveillance services [11].

The RT model, its characteristics, and details regarding its application to the problems under study in this work are described in Section 2. Validation results are illustrated in Section 3, where prediction performance is shown to be generally good, but very relevant and unexpected sources of error and inaccuracy are identified in several cases, as described in the different subsections, and possible solutions are also implemented and verified or proposed.

2. The Considered Ray-Based Model

2.1. The 3D Model's Basics. A 3D RT model developed at the University of Bologna has been used in the present work [13] and is shortly described in the following.

According to the deterministic approach, the RT engine requires to be fed by a detailed description of the urban environment. Geometrical information includes a vectorial representation of the building map, a digital description of the terrain height in raster format, and the positions of both the base station (BS) and the user equipment. In this work the BS will always be the transmitter (Tx) while the mobile stations will be the receiver (Rx). The electromagnetic description includes the antennas radiation patterns and the electromagnetic parameters of the materials, limited to the relative electrical permittivity (ε_R) and the conductivity (σ).

In order to reduce the amount of data to be stored and handled, and due to the common unavailability of a complete and detailed description of buildings, walls are simply represented as flat and smooth surface slabs. Based on such a simplified representation, coherent rays (i.e., involving canonical interactions like reflection/diffraction/transmission) are tracked through an "image-RT approach" according to Geometrical Optics (GO) theory [1] and to the Uniform Theory of Diffraction (UTD) [2].

To determine the propagating rays, the algorithm recursively sets up a so called "visibility tree," which is a virtual
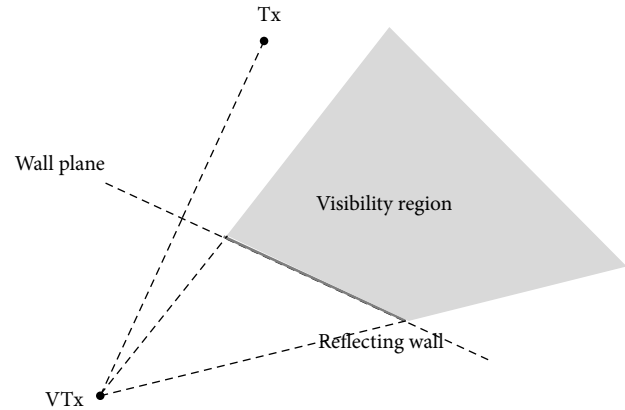

FIGURE 1: Example of VTx and visibility region for a reflecting wall.

layered structure representing the potential visibility relationships among transmitter, receiver, and interacting objects (i.e., walls and wedges) inside the scenario. In particular, objects are stored within the tree by means of proper "virtual transmitters" (VTx) that behave as secondary virtual sources [13, 14]. VTx locations related to wall-objects also depend on the electromagnetic interaction (reflection/transmission) experienced by the wall. For example, the first-order VTx associated with a wall is defined as the symmetric point (image) of the real Tx with respect to the wall plane if the wall acts as reflector (Figure 1), whereas it coincides with the Tx if transmission through the wall is assumed. A proper "visibility region" is also identified for each object, representing the spatial region that can be illuminated by the corresponding VTx. The visibility region of a reflecting wall is, for example, shown in Figure 1.

In order to reduce the computation time, only the objects included within the visibility region of each VTx are preselected and stored in the visibility tree.

The presence of a Rx inside the visibility region always means that an optical ray linking the Tx to the Rx exists, and its trajectory can be tracked climbing up the visibility tree according to a proper back-tracking procedure which determines the exact interaction points [9]. Of course, the undergone interactions must be compliant with the requirements preset at the beginning of the simulation: if the number of reflections/transmissions/diffractions exceeds the maximum allowed values, the ray must be discarded; otherwise, the field computation is performed. With reference to the number of transmissions, the ray-object intersection check is performed on the base of the Binary Space Partitioning approach [15].

In addition to standard electromagnetic interaction, the RT model also takes into account diffuse scattering (DS) due to building walls surface irregularities/volume dishomogeneities according to the "Effective Roughness" (ER) model [16]: the electromagnetic power impinging on a wall (or part of it) is spatially scattered according to a proper scattering coefficient *S* and a suitable, scattering pattern [16]. In order for the scattering model to be physically sound, diffusion occurs at the expense of reflected and transmitted powers, which are therefore properly reduced.

Differently from reflection, transmission, and diffraction, scattering is a "diffuse phenomenon"; that is, it can hardly be modelled by means of contributions coming from few, specific interaction points, as it is generated by a multitude of scatterers widely distributed on the scattering surface. According to this characteristic, the ER model requires the subdivision of each surface into "tiles" with prefixed dimensions; during the visibility assessment process, each tile is regarded as a single object with a VTx placed in its centre, which acts as secondary source of spherical wave radiated according to the scattering radiation pattern.

2.2. Extensions to the Ray Tracing Engine. Depending on the properties of the propagation scenario, the position of antennas (especially of BSs in cellular networks), and the link distance, the dominant propagation process can occur over building rooftops (ORT propagation), and/or around buildings along the street canyons [17]. Particularly when the BS antenna is placed near or above the rooftop level, propagation takes place primarily over the buildings [18], where the radio wave undergoes multiple diffractions over the horizontal edges delimiting the roofs contours.

Differently from the buildings vertical corners, horizontal edges are not necessarily parallel to each other, and this poses a theoretical limit to the computation of the multiple-diffracted field using a 3D ray tracing approach. In fact, although the geometrical trajectories can be tracked regardless of the number n_d of involved diffractions [19], analytical expressions for the corresponding propagating field are available only for n_d up to 3 if the wedges are arbitrarily oriented [20]. Since ORT propagation may sometimes require more than 3 diffractions, especially for large link distance, for rays undergoing more than 2 diffractions the fully 3D geometrical computation is replaced with a simplified approach using a multiple-screen UTD model limited to the vertical plane, considering one/two knife-edges for each building along the radial line between the Tx and the receiver (Rx). Before applying the UTD model, the ORT profile is simplified by identifying only the dominant obstacles with the "rubber-band" method. As discussed in Section 3, such multi-knife-edge models seem to overestimate the attenuation (see Section 3), probably due to the ideality of the knife-edge assumption with respect to the actual shape of buildings; some correction factors are therefore added depending on the number of knife-edges, as suggested in [21, 22].

A proper combination of ORT and diffuse scattering is also introduced in the model, since it led to a significant prediction improvement in some cases, as described in the next section. Since each scattering tile behaves as a secondary source for a new, spherical wave radiated in all directions, scattering or the combination of scattering and ORT seems to be efficient ways to reach non-line-of-sight (NLOS) Rxs in deep street canyons where diffraction from the roof edge is very weak, as depicted in Figure 2.

The RT tool has been also extended to take into account the effect of terrain, through ground reflection and obstruction. In the considered simulation setup, a Digital Terrain Model (DTM) consisting of a raster file with a resolution of 10 m is used.
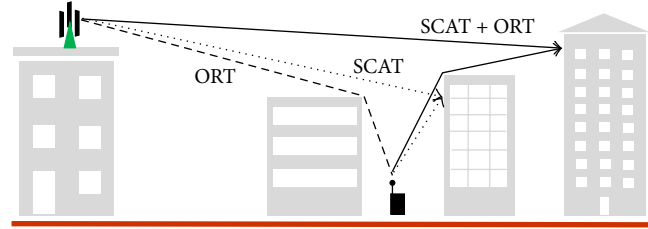

FIGURE 2: ORT model in the vertical plane and combination with scattering.

2.3. Impact of Computation Parameters. Preliminary evaluations have shown that a very high number of interactions is not necessary to get good predictions. In particular, the performance usually saturates (i.e., the mean error to tends to zero) when at least 3 reflections are considered, with the exception of high-rise building zones, where we found that a minimum number of 4 reflections are required. At least 2 diffractions (besides the ORT path) are necessary to obtain realistic predictions in the vicinity of street crossings. On the other hand, we found that increasing the number of diffractions from vertical edges above 2 does not improve NLOS propagation, especially for receivers located quite far from the line-of-sight (LOS) street crossings. Also through-building transmissions have been found to be important in some cases, especially for the buildings in proximity of the BSs. Finally, the impact of the diffuse scattering model and of its parameters on the model performance has been investigated: in particular, the area of the scattering tiles has been found to be a quite critical parameter which has to be set carefully, as illustrated in Section 3.

Investigations showed that results are not very sensitive to the building's material characteristics, as already highlighted in [23]. Ray tracing simulations were then performed with uniform material parameters (relative permittivity $\varepsilon_r = 5$, conductivity $\sigma = 0.02$ [S/m]), with a maximum of 4 reflections, 2 diffractions (also in combination with reflections), single-bounce diffuse scattering, and offline ORT combined with diffuse scattering as described above. Regarding the scattering parameter S, a value of 0.4 has been assumed for all building walls, in accordance with previous investigations' findings [16]. No material parameter optimization has been performed in the present work.

2.4. CPU Time Reduction. The required computational burden still represents a strong limitation to the widespread use of RT. The computational effort strongly depends on the number of objects (buildings) included in the input database, and it could be therefore reduced through an effective simplification of it. Such a speed-up technique is suggested in [12] and consists of the reduction of the input database by identifying and selecting the "active set" of buildings/obstacles (or "active map") and discarding the rest of the database. The "active set" consists of the buildings or obstacles that are actually involved in the propagation process. According to what was proposed in [12], the active map basically includes the buildings around and between

TABLE 1: Comparison between computation times and simulation results for site A000127C using full map and simplified map.

	Number of buildings	Computation time	% reduction in computation time	Mean prediction error[*]	Std. dev. of prediction error[*]
Full map	18050	≈3.5 days	—	—	—
Simplified map (standard method [12])	8706	≈1.5 days	58%	<0.1 dB	<0.1 dB
Simplified map (new method)	1923	≈10 hours	88%	<0.1 dB	<0.1 dB

[*]With respect to full-map prediction.

the radio terminals (inside an ellipse having Tx and Rx as focuses) and those in LOS with the Tx and/or the Rx. Moreover, buildings not directly visible from the terminals can be also involved in the propagation process, provided that they have considerable dimensions, height, and propitious orientation. In case both Tx and Rxs are positioned well above ground level (e.g., user equipment placed at upper floors of buildings), only the taller buildings among those around and between the terminals can be expected to affect radio propagation; a more effective map simplification could be therefore achieved using an ellipsoid instead of an ellipse, in order to avoid selecting low-rise, irrelevant buildings.

In this work, the huge sizes of the urban database and of the receiver's set impose the adoption of a drastic map simplification to keep computation time within reasonable limits of a few hours to a few days at most. Therefore only building and walls visible from *both* the Tx *and* the Rx have been selected outside of the mentioned ellipse.

In order to verify that the simplification algorithm does not cause a significant degradation of the results, some preliminary comparisons have been made between the simulation results obtained with the complete map, with the simplified map according to the "standard" method proposed in [12], and with the "drastic" simplification proposed in this paper. The results showed a significant reduction in computation time, with a negligible degradation of the results. As an example, in Table 1 these results are reported for site A000127C. The simulations were performed with the number of interactions recommended for low/medium-rise building zones (3 reflections, 2 diffractions, and single-bounce scattering), according to the investigations reported in Section 2.3.

In order to further reduce the computation time we decided to enable transmission through buildings only for the buildings located in the vicinity of the base station, that is, at distances lower than 100 m.

3. Validation Results

Eighteen 850 and 1900 MHz cell sites were chosen from all over the city of San Francisco. The cell site characteristics were derived from surveying each target site. BS antenna heights ranged from 6 to 100 m. Effective radiated power (ERP), which was found by using a scanner at LOS locations with each site, was generally between 30 and 45 dBm. On the receiver side, a Rhode Schwarz scanner was placed inside a minivan while a PCTEL OP178H omnidirectional antenna with 3 dBi gain was placed on top of the minivan. The

antenna height above the ground was approximately 1.8 m and exact Rx locations along routes were tracked using a combination of GPS, inertial devices, and speedometer. Using the scanner, the received signal strength indicator (RSSI) was recorded for the target broadcast control channels (BCCHs) as the minivan drove the streets around each cell site. From the recorded RSSI measurements, roughly 27,000 small-area average power measurements were extracted.

Given the huge size of the San Francisco digital map, thousands of buildings, millions of walls and edges, the environment was reduced to the minimum set of buildings really involved in the propagation process for each BS site using the method described in Section 2.4.

Computation time for 1 BS site was variable between 10 h and 2.5 days (depending on the site) on a single Xeon-CPU core of a PC. No special technique was adopted to reduce CPU time, but it is known that a great CPU time reduction is possible through parallelization on multiple CPU cores and/or Graphics Processing Units (GPU) or through cloud computing.

Performance is summarized in terms of mean error, error standard deviation, and RMS error in Table 2 for all 18 sites. Apart from a few sites for which particular conditions such as the presence of trees and traffic or uncertainties regarding the precise BS location degraded the results, as described below, performance is quite uniform with low mean errors and standard deviation of the errors of 7.3 to 9.7 dB.

Although the prediction error values reported in Table 2 are basically in line with the accuracy level commonly attributed to RT models, it is worth noticing that they have been here achieved in a really critical scenario, as stated in the introduction.

In Figure 3, the aggregate mean error and standard deviation of the error are reported for all sites as a function of distance from the BS, separating results corresponding to the LOS from those of the NLOS Rx locations. It is interesting to note that model's performance for both short distances and LOS receivers is not necessarily better than for long distances and NLOS receivers. This can be explained considering that while far/NLOS locations take advantage of a sort of "diversity gain" due to the presence of multiple propagating paths, close/LOS locations, where only one path is dominant, suffer from inaccuracies in the position and orientation of the BS antennas with respect to the surrounding obstacles and from the presence of obstacles such as big vehicles and trees, which are not described in the input database. The standard deviation shows a maximum for a distance of about 500 m and interestingly gradually drops to very small values for LOS

TABLE 2: Performance indicators for the 18 sites.

ID scenario	Short description	Number of Rxs	Mean error (dB)	Error std. dev. (dB)	RMS error (dB)
A00002E5	MC-UHR	563	4.70	13.00	14.00
A0000415	MC-UHR	1448	−2.74	7.72	8.20
A00005BA	SC-ULR	825	2.55	11.90	12.20
A0000A49	SC-ULR/UMR	1376	0.86	9.26	9.30
A0000DEF	SC-UMR	1044	−4.4	7.8	8.9
A0000F89	MC-UMR	1238	−3.00	9.54	10.00
A0000F8D	SC-ULR/UMR	923	−0.77	9.75	9.78
A0001137	SC-UMR	2126	1.46	8.47	8.60
A0001139	SC-UMR	1867	−2.64	8.90	9.30
A000127C	SC-UMR	1456	0.06	7.77	7.77
A00013B7	SC-UMR	1037	−5.13	7.60	9.17
A0001623	MC-UHR	1465	−2.70	8.71	9.12
A0001632	SC-UMR	532	3.80	11.30	12.00
A0001983	MC-UMR	1170	−2.00	8.28	8.53
A0001ABB	MC-UMR	1155	1.37	9.71	9.80
A0002FFC	SC-UMR	3139	1.30	7.35	7.47
A0003273	MC-UHR	2271	−9.40	9.88	13.70
A00034F4	MC-UHR	3074	−5.20	11.59	12.70

Categories of sites and environment: small cell (SC)/macrocell (MC); urban low rise (ULR)/urban medium rise (UMR)/urban high rise (UHR).
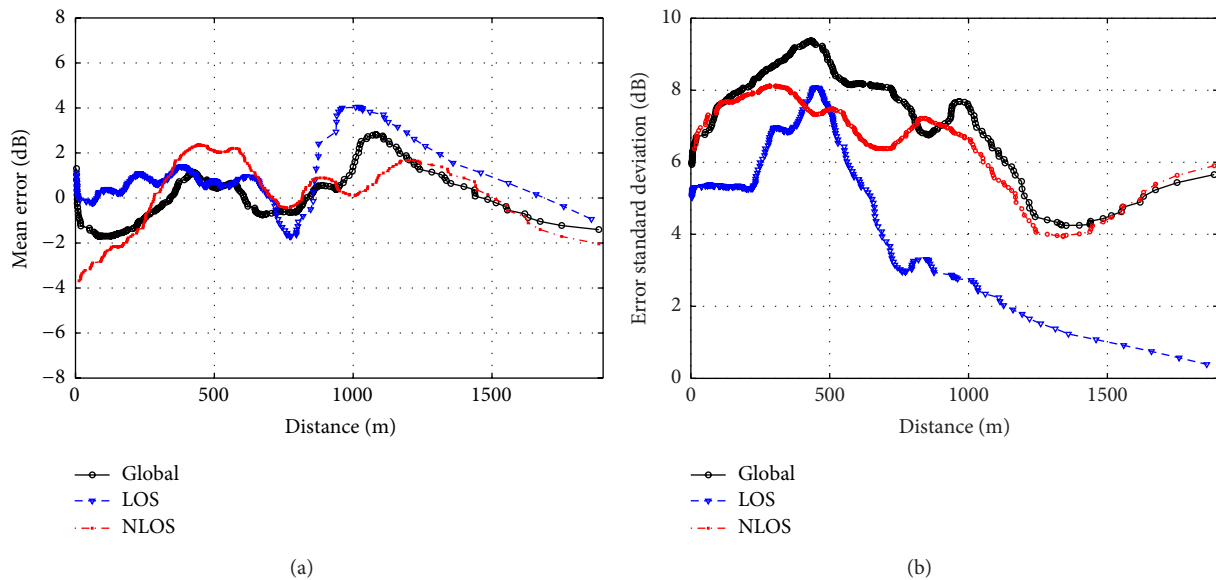

FIGURE 3: Mean error (a) and standard deviation of the error (b) for all sites and for LOS and NLOS Rx locations.

locations, while it remains higher for NLOS locations. The mean error on the contrary seems to tend toward negative values for high distances, especially in NLOS locations, probably due to an underestimation in the ORT model as explained in Section 3.3.

In Figure 4, mean error and standard deviation of the error are reported for high-rise and medium/low-rise sites. As expected performance is poorer, with strongly negative mean error and consistently high standard deviations, for high-rise areas, where the presence of very tall buildings with irregular heights strongly affects the wave propagation, which would probably require a higher number of interactions to be accurately described.

A more detailed analysis of the major causes of errors in RT predictions and of the possible countermeasures is reported in the following subsections.
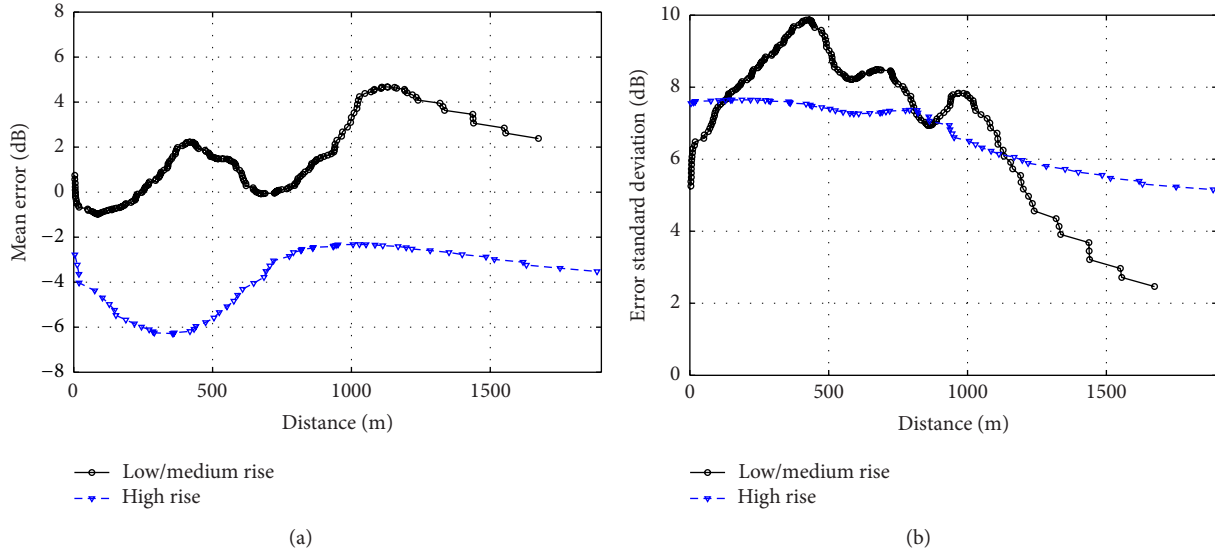
FIGURE 4: Mean error (a) and standard deviation of the error (b) for low/medium-rise (black) and high-rise (blue) environments.

3.1. Inaccuracies in the BSs Position. After a careful analysis of the RT output, visual inspection of the BS locations both "on site" and using internet-based tools such as Google Street View, we found that a major source of error is related to the inaccuracy of the environment representation within the digital database and above all to the mismatch between the available information on coordinates and orientation of the BS antennas and the representation in the digital map of the buildings where the antennas are mounted on, or in their proximity. Due to the size and complexity of the urban environment, the digital building map is often acquired from specialized vendors and therefore it is usually quite accurate in itself. However, database accuracy is hardly better than 0.5 m for horizontal coordinates and often worse for vertical coordinates (e.g., buildings heights), due to the somehow rough shape approximation of the rooftops [13]. Such inaccuracies can be especially critical if referred to the buildings in close proximity of the antennas that can dramatically modify the visibility relations. Furthermore, additional errors are often present in the data describing the antenna's position and radiation pattern. Such information is often drawn from technical documentation released by the mobile radio operators, which might be out-of-date and not fully reliable. According to the available information one of the BSs was declared as having the height of 46 m, whereas it was actually mounted on top of building at a height of 100 m! Such wrong data initially produced a poor simulations performance (mean error of −8.7 dBm), later improved correcting BS height (mean error dropped to −2.74 dBm). This of course represents a very extreme case, but an inaccuracy of just a few meters in the position of the BS antenna with respect to the near-by building can make the difference between a below-roof case and an above-roof case, with an obvious dramatic impact on propagation conditions. Correcting BS position information is a possible, albeit very time-consuming task, that not always leads to

smaller errors as will be shown in Section 3.3. Regarding the 18 cell sites chosen for the model validation, 4 of them required significant corrections for the BS position, while the information for the remaining 14 sites were reliable.

3.2. Urban Cluttering. Another important source of error, unexpected in such evident terms, is the effect of street cluttering (vehicles, street signs, poles, lamp-posts, trees, etc.). Unlike accurate BS position, cluttering can hardly be described in the environment database due to its variability. Cluttering has been shown to have a twofold effect:

(a) additional obstruction along street canyons;

(b) scattering at street intersections.

While (a) adds excess attenuation and results in overestimations, especially in LOS street canyons, (b) enhances beyond-street-corner propagation thus reducing street-corner loss, as already discussed in recent publications [24]. The two effects are evident in Figure 5 where the error (predicted-measured RF coverage [dB]) is shown for site A0000F8D in a color-scale map. While the error is increasingly positive along LOS street canyons, probably due to the presence of vegetation and parked vehicles, it abruptly drops to negative values (see zone highlighted in yellow) in NLOS side streets.

Although the problem related to the street corners has not been practically addressed so far, a possible solution may consist of the introduction of proper scatterers in the middle of the street intersections to simulate the effect of cluttering. An alternative/complementary approach may refer to the use of diffraction coefficients for conducting wedges to partly compensate the lack of scattering from clutter by means of artfully boosted diffracted contributions.

Problem (a) has been empirically reduced through the introduction of a correction factor in LOS-Rx simulations for

FIGURE 5: Map of the error [dB] for site A0000F8D. BS position is shown as a black dot.

−4 dB/100 m in red zone
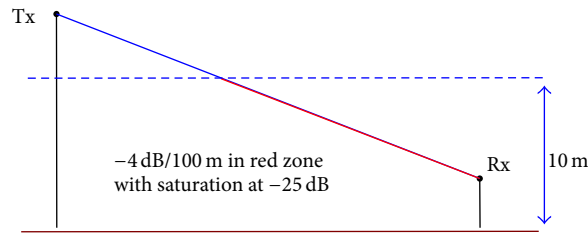with saturation at −25 dB

Tx

Rx

10 m

FIGURE 6: Correction factor adopted for LOS-Rx.

LOS and single-bounce rays. As represented in Figure 6, ray power has been reduced by 0.04 dB/m for rays propagating below the height of 10 m with a ceiling of 25 dB. Unfortunately this action does not fully compensate the LOS overestimation.

The effectiveness of the expedient sketched in Figure 6 is still unsatisfactory in street canyon affected by a dense clutter. In such cases a further improvement of the prediction accuracy along the canyons has been achieved by simply discarding all the rays except the direct one (see Figure 7). In the shown example (site A0000A49), there is an evident overestimation of the power when rays undergoing multiple interactions in the street canyon are included in the simulation (Figure 7(a)), while a significant reduction of the error is obtained including only the LOS ray (Figure 7(b)). From a physical point of view, this solution can be somehow explained considering the fact that urban clutter might in some cases prevent the multiple reflected/diffracted paths from giving a relevant contribution to received power.

However the best solution would be a systematic introduction within the RT algorithm of correction factors for all rays propagating in all streets lined by trees or cluttered with buses and traffic.

3.3. Impact of Scattering Tiles Dimensions. Owing to its distributed nature (already discussed in Section 2.1), an accurate modelling of DS would clearly benefit from dividing walls surfaces into tiny surface elements, but that would mean a huge number of scattering VTx and thus a strong increase in the computational burden. A trade-off must be made here.

Alternatively, this problem can be bypassed by modelling the scattering generated by very large buildings through analytical formulas, according to the approach proposed in [25, 26], thus obtaining an arbitrarily large resolution. However, according to our experience, a division of the walls into surface elements with areas of some tens of square meters, is already sufficient to obtain good results with no significant increase of the computation time.

The sensitivity of the prediction accuracy to the dimension of the scattering tiles is highlighted in Figure 8 for site A0000DEF, where some Rx locations are placed close to the Transamerica Pyramid (Figure 8(a)), the tallest skyscraper in San Francisco. Due to its large dimension, such building intercepts part of the energy radiated by the BS (Figure 8(b)) and directly backscatters the signal to the receivers at street level. According to the ER approach, the scattered wave springs out from the tiles centre according to a scattering radiation pattern with a main lobe steered around the direction of specular reflection [16]. If the walls subdivision is too rough, no scattering VTx close to the street level are present, and the scattering radiation lobes are therefore never oriented towards the Rxs near to the Pyramid. This results in a strong underestimation of the RSSI. In the considered case, a satisfactory prediction in the vicinity of the Pyramid is achieved by dividing its walls in tiles of size 15 × 15 m (see Figure 8(d)), compared to the "rough" case where a single scattering VTx is placed in the barycentre of each wall (Figure 8(c)).

Moreover in Figure 8, the effect of the BS position updating is present. In particular, this can be noted in the

(a)

(b)

FIGURE 7: Impact of the ray selection method in urban street canyons: (a) error map [dB] obtained including rays with multiple reflections/diffractions; (b) error map obtained including only LOS ray in the street canyon [site A0000A49; BS position is shown as a black dot].

upper part of Figure 8(d), where the effect of the actual position of the BS site provides a smaller error along the diagonal street, but a higher error in the quasi-horizontal street. This further confirms what is already discussed in Section 3.1, namely, that the positioning of BS with respect to the environment is particularly critical, and inaccuracies of a few tens of centimeters or meters can cause substantial differences in the simulation results.

3.4. ORT Propagation Modelling. Other important sources of errors are related to the irregularity of the San Francisco urban layout which has a large variety of building heights and shapes and a very hilly terrain. To our great surprise, well-established ORT models based on multiple knife-edge (KE) diffraction, including multiple-diffraction UTD models in the vertical plane and others we have tested, appeared to strongly underestimate RF coverage and the errors increase with the number of involved obstacles. To assess this problem we selected "strongly NLOS" Rx locations with link-distance $d > 650$ m, where ORT propagation is dominant with respect to propagation along street canyons. Predictions were then performed with a multiple-diffraction UTD model and compared to measurements at the selected locations. Results are shown in Figure 9: errors of the order of some tens

of dB are observed even for a low number of KEs (2 or 3). This behaviour is probably related to the very irregular urban layout of central San Francisco, where many tall and narrow buildings are scattered everywhere: such buildings can hardly be represented by KEs, as most of the power can actually diffract *around* the building, while a KE only allows the signal to pass *over* the building top with a much greater power loss. Therefore correction factors dependent on the number of KE should be introduced in irregular building layouts. Correction factors adopted in the Italian National Reference Propagation Models have been considered here [21, 22], although these turned out to undercompensate the error. As an alternative 3D propagation models such as Fourier's Optics or the Parabolic Equation Method could be applied.

Last but not least, we found that diffuse scattering *combined* with ORT propagation, a combination usually neglected in ray-based prediction tools, represents one of the dominant propagation mechanisms in hilly terrain cases, especially for coverage in built-up, elevated areas on hills. This point has been already addressed in Section 2.2 and partly explained through Figure 2. As an example, the difference of the RF coverage prediction error obtained with a conventional RT simulation (including separately ER diffuse scattering and ORT) and with RT simulation including the
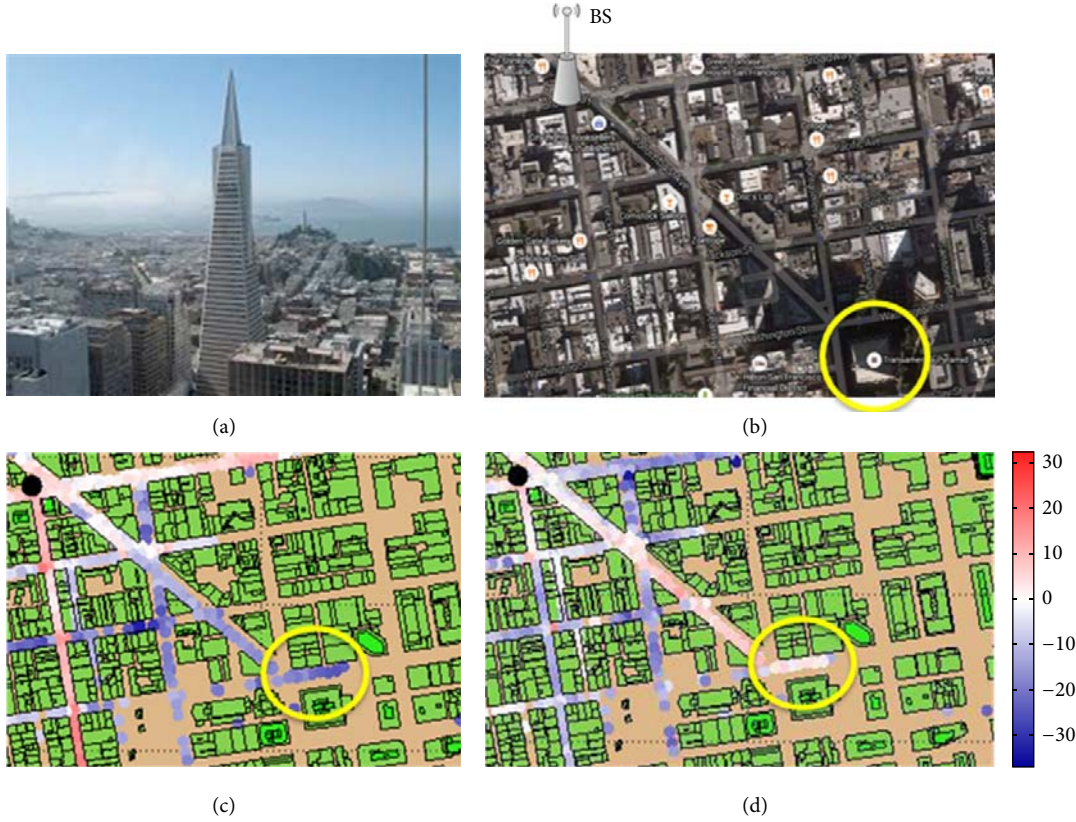
FIGURE 8: Prediction error with rough (c) and improved (d) walls subdivision in tiles [site A0000DEF; BS position is shown as a black dot].
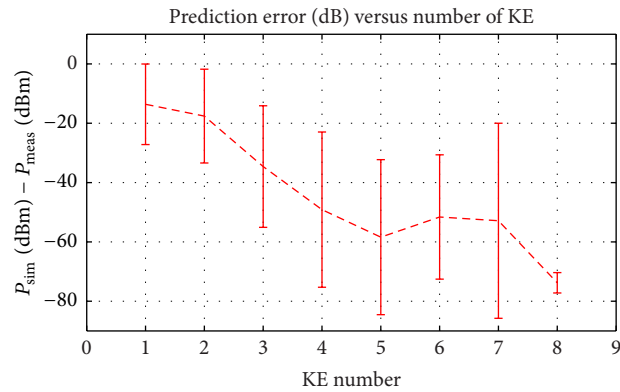

FIGURE 9: ORT model error [dB] for selected strongly NLOS and "far" Rx positions.

combination of ORT and ER scattering is shown in Figure 10 for site A0002FFC. It is evident that conventional RT strongly underestimates coverage (blue colour), especially in the hilly area in the upper part of the map. This fact needs further investigation: probably power propagating over the rooftops does not only propagate radially, but it seems to back-scatter on prominent buildings that stand out due to their height before descending to the Rx into the street. In Table 3, the concise performance parameters (mean error, error standard deviation, and root-mean-square error) are also reported for the same site.

4. Conclusions

A very extensive validation of an advanced 3D ray tracing model is carried out through comparison with measurements in one of the most challenging environments: the city of San Francisco. Although narrowband propagation at UHF frequencies has been widely studied in the last 20 years, we show that there is still a wide margin of improvement. Very relevant sources of error and inaccuracy are identified in several cases, including the effect of inaccuracies in the position and orientation of base station antennas, the underestimation

Error (prediction-measurement) (dB)

Conventional RT simulation   With diffuse scattering + ORT
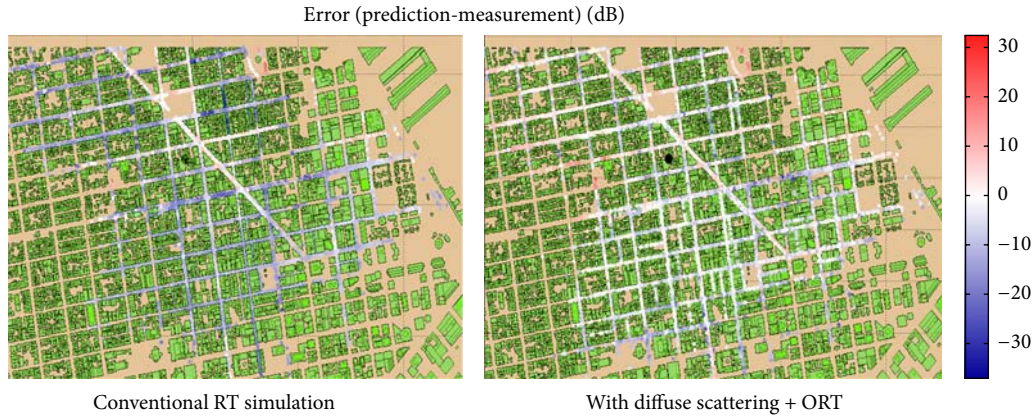
FIGURE 10: Comparison of RF coverage prediction error between conventional RT simulation (with ORT model included) and RT simulation with scattering *combined* with ORT; site A0002FFC.

TABLE 3: Comparison between results with different ORT models (site A0002FFC).

	Mean error (dB)	Error standard deviation (dB)	RMS error (dB)
Standard ORT model	−9.267	13.7	10.08
ORT with correction factors	−9.045	13.32	9.775
ORT with correction factors and combined with scattering	1.3	7.32	7.44

of conventional multi-knife-edge diffraction models, the effect of street cluttering, and the effect of diffuse scattering combined with ORT propagation. Possible solutions to the mentioned problems are proposed, and some of them are implemented and assessed in this study.
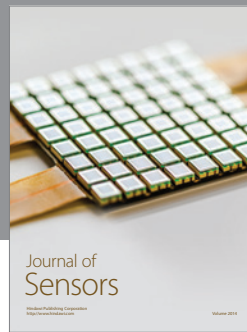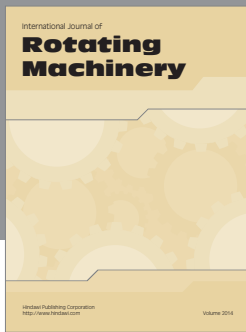
Conflict of Interests

The authors declare that there is no conflict of interests regarding the publication of this paper.

References

[1] L. B. Felsen and N. Marcuvitz, *Radiation and Scattering of Waves*, Prentice Hall, 1973, IEEE Press, 1994.

[2] R. G. Kouyoumjian and P. H. Pathak, "A uniform geometrical theory of diffraction for an edge in a perfectly conducting surface," *Proceedings of the IEEE*, vol. 62, no. 11, pp. 1448–1461, 1974.

[3] J. Walfisch and H. L. Bertoni, "A theoretical model of UHF propagation in urban environments," *IEEE Transactions on Antennas and Propagation*, vol. 36, no. 12, pp. 1788–1796, 1988.

[4] K. Rizk, J.-F. Wagen, and F. Gardiol, "Two dimensional ray tracing modeling for propagation prediction in microcellular environments," *IEEE Transactions on Vehicular Technology*, vol. 46, no. 2, pp. 508–518, 1997.

[5] G. Liang and H. L. Bertoni, "A new approach to 3-D ray tracing for propagation prediction in cities," *IEEE Transactions on Antennas and Propagation*, vol. 46, no. 6, pp. 853–863, 1998.

[6] S.-C. Kim, B. J. Guarino Jr., T. M. Willis III et al., "Radio propagation measurements and prediction using three-dimensional ray tracing in urban environments at 908 MHz and 1.9 GHz," *IEEE Transactions on Vehicular Technology*, vol. 48, no. 3, pp. 931–946, 1999.

[7] J.-P. Rossi and Y. Gabillet, "A mixed ray launching/tracing method for full 3-D UHF propagation modeling and comparison with wide-band measurements," *IEEE Transactions on Antennas and Propagation*, vol. 50, no. 4, pp. 517–523, 2002.

[8] T. Kürner and A. Meier, "Prediction of outdoor and outdoor-to-indoor coverage in urban areas at 1.8 GHz," *IEEE Journal on Selected Areas in Communications*, vol. 20, no. 3, pp. 496–506, 2002.

[9] V. Degli-Esposti, D. Guiducci, A. de'Marsi, P. Azzi, and F. Fuschini, "An advanced field prediction model including diffuse scattering," *IEEE Transactions on Antennas and Propagation*, vol. 52, no. 7, pp. 1717–1728, 2004.

[10] Y. Corre and Y. Lostanlen, "Three-dimensional urban EM wave propagation model for radio network planning and optimization over large areas," *IEEE Transactions on Vehicular Technology*, vol. 58, no. 7, pp. 3112–3123, 2009.

[11] J. Zhu, S. Spain, T. Bhattacharya, and G. D. Durgin, "Performance of an indoor/outdoor RSS signature cellular handset location method in Manhattan," in *Proceedings of the IEEE Antennas and Propagation Society International Symposium*, pp. 3069–3072, IEEE, Albuquerque, NM, USA, July 2006.

[12] V. Degli-Esposti, F. Fuschini, E. M. Vitucci, and G. Falciasecca, "Speed-up techniques for ray tracing field prediction models," *IEEE Transactions on Antennas and Propagation*, vol. 57, no. 5, pp. 1469–1480, 2009.

[13] F. Fuschini, E. M. Vitucci, M. Barbiroli, G. Falciasecca, and V. Degli Esposti, "Ray tracing propagation modeling for future small-cell and indoor applications: a review of current techniques," *Radio Science*, vol. 60, no. 6, pp. 469–485, 2015.

[14] M. G. Sánchez, L. de Haro, A. G. Pino, and M. Calvo, "Exhaustive ray tracing algorithm for microcellular propagation prediction models," *Electronics Letters*, vol. 32, no. 7, pp. 624–625, 1996.

[15] A. S. Glassner, "Space subdivision for a fast ray tracing," *IEEE Computer Graphics and Applications*, vol. 4, no. 10, pp. 15–22, 1984.

[16] V. Degli-Esposti, F. Fuschini, E. M. Vitucci, and G. Falciasecca, "Measurement and modelling of scattering from buildings," *IEEE Transactions on Antennas and Propagation*, vol. 55, no. 1, pp. 143–153, 2007.

[17] F. Fuschini, V. Degli-Esposti, and G. Falciasecca, "A statistical model for over rooftop propagation," *IEEE Transactions on Antennas and Propagation*, vol. 52, no. 1, pp. 230–239, 2004.

[18] H. L. Bertoni, *Radio Propagation for Modern Wireless Systems*, Prentice Hall, 2000.

[19] G. Carluccio and M. Albani, "An efficient ray tracing algorithm for multiple straight wedge diffraction," *IEEE Transactions on Antennas and Propagation*, vol. 56, no. 11, pp. 3534–3542, 2008.

[20] G. Carluccio, F. Puggelli, and M. Albani, "A UTD triple diffraction coefficient for straight wedges in arbitrary configuration," *IEEE Transactions on Antennas and Propagation*, vol. 60, no. 12, pp. 5809–5817, 2012.

[21] Working Group of the Ministry of Communications, "National Model for the verification of the coverage of cellular mobile radio systems," ISPT Internal Report, 1996, (Italian).

[22] M. Frullone, P. Grazioso, G. Riva, and A. M. Serra, "Evaluation of diffraction losses over multiple obstacles for field strength prediction," in *Proceedings of the International Symposium on Broadcasting Technology*, pp. 311–316, Zhuhai, China, August 1991.

[23] G. E. Athanasiadou and A. R. Nix, "Investigation into the sensitivity of the power predictions of a microcellular ray tracing propagation model," *IEEE Transactions on Vehicular Technology*, vol. 49, no. 4, pp. 1140–1151, 2000.

[24] M. Ghoraishi, J. Takada, and T. Imai, "Radio wave scattering from lampposts in microcell urban mobile propagation channel," *ECTI Transactions on Electrical Engineering, Electronics, and Communications*, vol. 7, no. 1, pp. 14–20, 2009.

[25] V. Degli-Esposti, F. Fuschini, and E. M. Vitucci, "A fast model for distributed scattering from buildings," in *Proceedings of the 3rd European Conference on Antennas and Propagation (EuCAP '09)*, pp. 1932–1936, Berlin, Germany, March 2009.

[26] V. Degli-Esposti, F. Fuschini, and E. M. Vitucci, "Implementation of a fast distributed scattering model for Ray Tracing prediction," in *Proceedings of the 7th European Conference on Antennas and Propagation (EuCAP '13)*, pp. 3039–3042, IEEE, Gothenburg, Sweden, April 2013.